14th Australasian Fluid Mechanics Conference
Adelaide University, Adelaide, Australia
10-14 December 2001

Drag Coefficient for Arrays of Cylinders in Flows of Power-Law Fluids

P. D. M. Spelt[1], T. Selerland[1], C. J. Lawrence[2] and P. D. Lee[3]

[1]Centre for Composite Materials, Imperial College, London, SW7 2BY, UNITED KINGDOM
[2]Department of Chemical Engineering, Imperial College, London, SW7 2BY, UNITED KINGDOM
[3]Department of Materials, Imperial College, London, SW7 2BP, UNITED KINGDOM

Abstract

Numerical simulations are presented of flows of power-law fluids through periodic arrays of aligned cylinders, both creeping flows and flows with finite inertia. Results are presented for the drag coefficient of the cylinders and are compared against asymptotically valid analytical results. Square and hexagonal arrays are considered, both for flow in the plane perpendicular to the alignment vector of the cylinders (along the axes of the array as well as off-axis flows), and for flow along the cylinders. It is shown that the observed strong dependence of the drag coefficient on the power-law index (through which the stress tensor is related to the rate-of-strain tensor) for creeping flows can be described at all solid area fractions by scaling the drag on a cylinder with appropriate velocity and length scales. For flows with finite inertia a similar scaling is found.

Introduction

The creeping flow of Newtonian fluids through periodic arrays of cylinders has been studied extensively [7, 2] mainly because of its importance in many applications in heat and mass transfer equipment. More recently the corresponding flows with small-but-finite and intermediate Reynolds number have been studied (Edwards *et al.* [3], Ghaddar [4] and Koch and Ladd [5]).

The literature on non-Newtonian fluid flows through periodic arrays of cylinders is far less complete, although these problems have now become of great practical relevance with the increasing popularity of polymer composite materials. The manufacture of these materials often involves flow of polymer resin through fibrous materials, as for instance in the resin transfer moulding process (RTM), in which a polymer resin is injected into a mould which contains a fibrous preform. The fibres are often bundled together in dense strands.

The rheology of many non-viscoelastic non-Newtonian fluids can be approximated by the power-law fluid model, i.e., by supposing the stress to be proportional to the shear rate to the power n, where n is the power-law index [8]. Creeping flows of power-law fluids through periodic arrays were simulated by Bruschke and Advani [1] for (transverse) flow in the plane normal to the alignment vector of the cylinders. Sadiq, Advani and Parnas [6] carried out a variety of experiments with power-law fluids (with $0.39 \leq n \leq 0.54$) in square arrays of solid rods, as well as arrays of fibre bundles. Vijaysri *et al.* [12] used a cell model in their simulations of power-law fluid flows through arrays of cylinders.

The aim of the present contribution is to extend the previous work on flows of power-law fluids through arrays of cylinders to off-axis flows (flows in the plane perpendicular to the alignment vector of the cylinders, but with the main flow direction not aligned with an axis of the array) and to investigate the effect of finite fluid inertia.

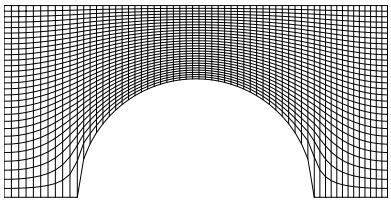

Figure 1: An example of a mesh used for square arrays (area fraction $\phi = 0.3$); only the bottom half of the actual mesh is shown. The computational mesh points are located at the cell centres.

Method

The flow of power-law fluids is governed by the following equations of motion, where $\boldsymbol{V}$ is the velocity vector, P is the pressure, $\boldsymbol{\tau}$ is the viscous part of the stress tensor, and ρ is the density:

$$\frac{\partial V_j}{\partial x_j} = 0, \quad \rho\frac{\partial V_i}{\partial t} + \rho\frac{\partial}{\partial x_j}\left(V_i V_j\right) = -\frac{\partial P}{\partial x_i} + \frac{\partial \tau_{ij}}{\partial x_j}. \quad (1)$$

For a power-law fluid the viscous part of the stress tensor depends on the rate-of-strain tensor through [8]

$$\tau_{ij} = 2K\Pi^{(n-1)/2}E_{ij}, \quad E_{ij} = \frac{1}{2}\left(\frac{\partial V_i}{\partial x_j} + \frac{\partial V_j}{\partial x_i}\right), \quad (2)$$

where $\Pi = 2E_{kl}E_{kl}$ is the second invariant of the rate-of-strain tensor (where summation over the indices k and l is presumed). K and n are the power-law coefficient and index, respectively. $n = 1$ corresponds to a Newtonian fluid and $n > 1$ to a shear-thickening fluid.

The above equations of motion have been integrated numerically to a steady state for flow through a periodic array over which a pressure drop is imposed. A typical mesh is shown in Figure 1. The finite-difference, fractional step method of Zang, Street and Koseff [14] has been adopted for this purpose; details of the implementation of the non-linear stress tensor in this method will be published in Spelt *et al.* [9].

Results for creeping flows

The applied pressure drop over a unit cell of the array is balanced by the drag force applied to the cylinder in the cell. A simple scaling is used to introduce the drag coefficient C_d,

$$F \equiv C_d(\phi, n)Ka^{1-n}U^n, \quad (3)$$

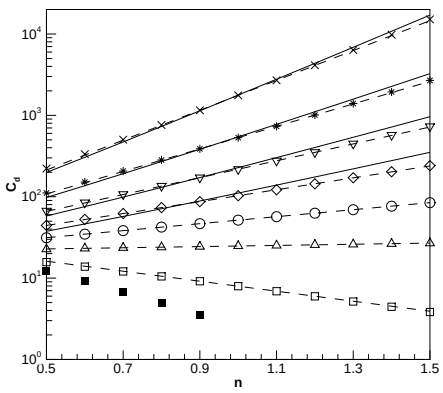

Figure 2: The drag coefficient C_d of a cylinder in a square (a) and hexagonal (b) array as a function of power-law index n for square arrays at area fractions 0.01 ($\Box$), 0.1 (Δ), 0.2 ($\bigcirc$), 0.3 ($\diamond$), 0.4 (∇), 0.5 ($*$) and 0.6 ($\times$). The filled symbols are numerical simulation results by Tanner [11] for a single cylinder in an infinite medium. The solid lines represent the lubrication theory (4). The dashed lines are (5).

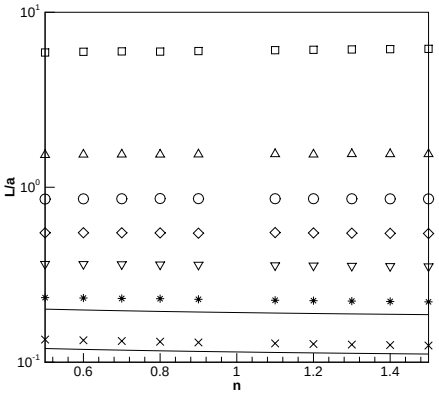

Figure 3: Numerical simulation results for the ratio L/a defined by (5) for a cylinder in a square array as a function of power-law index n at different area fractions. Symbols as in Figure 2. The lines correspond to the lubrication theory (4).

where F is the applied force per unit length of cylinder and a is the cylinder radius. Because F is simply the product of the applied pressure drop over the cell and the area of the face normal to the flow, and is therefore known, the drag coefficient is obtained from (3) by calculating the magnitude of the cell-averaged fluid velocity U.

On-axis flows

C_d as a function of power-law index n for on-axis creeping flows through square arrays is shown in Figure 2, at different solid area fractions ($\equiv \phi$) of the array. The results for $n = 1$ (the Newtonian case) agree very well (within 2%) with Sangani & Acrivos' [7] results and show the expected trend of a strong increase of C_d with ϕ.

The results are shown together with a lubrication theory for concentrated arrays. At high solid area fraction the pressure drop over the unit cell is mainly due to the fact that the fluid has to be forced through the narrow gap between the cylinders. Following the usual procedure the pressure drop can be calculated from which the following expression for the drag coefficient is obtained:

$$C_d = 2^{\frac{3}{2}}\pi^{\frac{1}{2}}\left(\frac{1+2n}{n}\right)^n \times \frac{\Gamma(2n+\frac{1}{2})}{\Gamma(2n+1)}\left(1-\left(\frac{\phi}{\phi_{\max}}\right)^{1/2}\right)^{-2n-1/2} \quad (4)$$

for cases in which $|\phi - \phi_{\max}| \ll 1$, where $\phi_{\max} = \pi/4$ is the maximum possible solid area fraction. The result for hexagonal arrays is essentially the same as (4), but with an additional factor of $3^{n/2+1/2}/2^n$ on the right-hand side and with $\phi_{\max} = \pi/(2\sqrt{3})$. The agreement of the simulation results with (4) is seen to be excellent at high ϕ.

Also seen from Figure 2 is the very strong dependence of C_d on n. The variation of the drag coefficient with n depends of course on the way in which the drag coefficient is defined in the first place. We use (3) here because it coincides for $n = 1$ with the definition used in the literature for Newtonian fluids and is an obvious extension of it. However, scaling the shear rate with the velocity averaged over the unit cell and the cylinder radius introduces a dependence of C_d on n because the actual shear rate (in Π, see (2)) in the gap between the cylinders scales with the ratio of a velocity scale $U_L \equiv Uc/L$ (with c half the height of the unit cell) and a length scale L, which are probably not too different from the averaged velocity in the gaps between the cylinders and half the gap size.

Using these instead to scale the 'viscosity', a different drag coefficient can be introduced (as in (3)) which, in general, will depend on n as well as on ϕ. Defining L so that this new drag coefficient does not depend on n, and equating both scaling relations of the drag force, the drag coefficient defined by (3) is found to have the following dependence on n:

$$C_d(\phi, n) \equiv C_d(\phi, 1)\left(\frac{\phi_{\max}}{\phi}\right)^{(n-1)/2}\left(\frac{L}{a}\right)^{2-2n}. \quad (5)$$

The value of L/a thus equals the ratio $(C_d(\phi,n)/C_d(\phi,1))^{1/(2-2n)}$. In Figure 3 the numerical simulation results for L/a have been plotted. If the above argument is all there is to the dependence of the drag coefficient seen in Figure 2 on n, then L/a should be a function of ϕ only. We see that this is indeed the case. After averaging L/a for each ϕ over the whole range of n equation (5) has been used to plot the values for C_d in Figure 2 (the dashed lines). We also see from Figure 2 that Tanner's [11] results for the drag coefficient of a single cylinder follow a similar scaling. We found that those results can be approximated by using $L/a \approx 19$.

The results for the drag coefficient of cylinders in a hexagonal arrangement showed the same trends. The same is also true for the case of flow along the cylinders. The resulting values of the ratio L/a for all these cases turned out to be virtually independent of n. Values of L/a averaged over n are shown as functions of ϕ in Figure 4.

Off-axis flows

For creeping flows of Newtonian fluids through square and hexagonal arrays the drag coefficient is independent

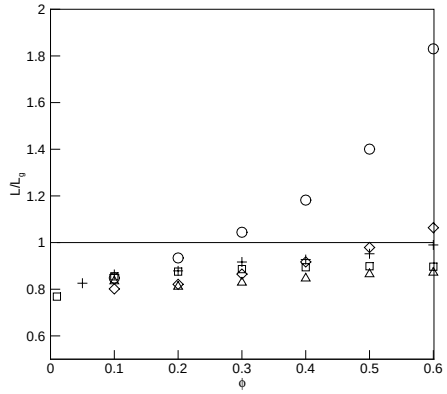

Figure 4: L obtained from averaging the numerical simulation data at each area fraction over all n, as a function of area fraction ϕ. (□), on-axis transverse flow, square arrays; (Δ), on-axis transverse flow, hexagonal arrays; (◯), longitudinal flow, square arrays; (⋄), longitudinal flow, hexagonal arrays; (+), on-axis transverse flow, square arrays (inferred from Bruschke and Advani [1]). L_g is the minimum size of the gap between the cylinders.

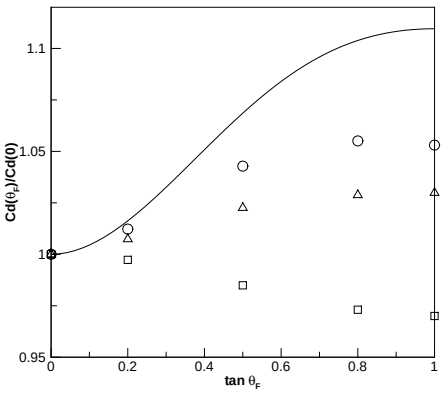

Figure 5: The ratio of the drag coefficient for off-axis transverse flow with $n = 0.7$ through square arrays divided by the on-axis drag coefficient as a function of the tangent of the angle θ_F the applied pressure drop makes with the nearest axis of the array at different area fractions: (□), $\phi = 0.1$; (Δ), $\phi = 0.3$; (◯), $\phi = 0.5$. The line is the result from lubrication theory.

of direction of the main flow. For general power-law fluids the equations of motion are not linear and no isotropy of the drag coefficient is expected and the cell-averaged velocity is not necessarily aligned with the drag force.

C_d for off-axis flows through square arrays is shown in Figure 5 for $n = 0.7$. The drag is seen to increase if the flow is less aligned with the axes of the array, simply approaching the lubrication theory when ϕ is increased. This increased drag magnitude is accompanied by a tendency for the cell-averaged velocity to be more aligned with the nearest axis of the array than the drag force. Again, the results are seen to be in agreement with a lubrication theory (the full lubrication theory is presented in Spelt *et al.* [9]). These trends are caused by the non-linear dependence of the pressure drop on the fluid velocity: for gaps over which the pressure drop is smaller, the resulting flow is smaller by a greater factor.

Inertial effects

Writing the equations of motion of power-law fluids in dimensionless form yields the Reynolds number $Re_a \equiv \rho a^n U^{2-n}/K$, with a the radius of the cylinders. It can be shown that the correction to the drag coefficient due to small-but-finite inertial effects can be written in the form (Spelt *et al.* [10])

$$C_d(\phi, n, Re_a) = k_0(\phi, n) + k_2(\phi, n) Re_a^2 + ..., \ (Re_a \ll 1), \tag{6}$$

which is a generalisation of the result for Newtonian fluids ($n = 1$) derived by Koch and Ladd [5].

Numerical simulations were carried out at different pressure drops, resulting in different Reynolds numbers, and a regression analysis was applied to find the proportionality constant k_2 for each ϕ and n. The results are shown in Figure 7. A strong dependence on the power-law index n is observed. However, as with the creeping flow results, part of this is due to using the cylinder radius a in the scaling of the drag force. The other part turns out to be due to using a in the definition of the Reynolds number.

We therefore introduce first a drag coefficient $\tilde{C}_d$ based on L and U_L, as above. An expansion similar to (6) holds for $\tilde{C}_d$. Further, we replace the Reynolds number in this expansion by $\widetilde{Re}$, which is based on a viscosity scale $\eta_H \equiv K(U_H/H)^{n-1}$, where $H(\phi, n)$ is a length scale and $U_H = Uc/H$ a velocity scale. We shall denote the new proportionality constant in the revised (6) by $\hat{k}_2(\phi, n)$ We shall now define $H(\phi, n)$ such that $\hat{k}_2(\phi, n)$ does not depend on n. We can obtain $H(\phi, n)$ from the simulation results through

$$\frac{H(\phi, n)}{a} = \left(\frac{k_2(\phi, n)}{k_2(\phi, 1)}\right)^{1/(4n-4)} \left(\frac{\phi_{\max}}{\phi}\right)^{1/8} \left(\frac{L(\phi)}{a}\right)^{1/2}. \tag{7}$$

The results are shown in Figure 8. We see that H only weakly depends on the power-law index and that H is larger than L for concentrated arrays.

Conclusions

Numerical simulation results have been presented for the flow of power-law fluids through arrays of cylinders, in terms of the drag coefficient of a cylinder in the array. Both flow in the plane perpendicular to the alignment vector of the cylinders and flow along the cylinders have been simulated. Creeping flow and flows with finite inertia were studied. It has been shown that despite the strong non-linearity of the equations of motion, the results for the drag coefficient can be explained with simple scaling arguments.

Future work will focus on the simulation of a fluid interface passing through the array. We shall adopt the level-set method to track the front position. Also, we have carried out simulations of power-law fluid flow through arrays of ellipsoidal cylinders [13].

References

[1] Bruschke, M.V. and Advani, S.G., Flow of generalized Newtonian fluids across a periodic array of cylinders, *J. Rheol.*, **37**, 1993, 479–498.

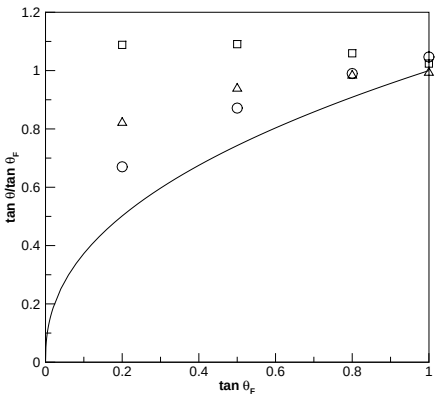

Figure 6: The ratio of the tangent of the angle θ that the averaged velocity makes with the nearest axis of the array and the tangent of the angle θ_F that the applied pressure drop over the array makes with the nearest axis of the array as a function of the tangent θ_F. Symbols as in Figure 5.

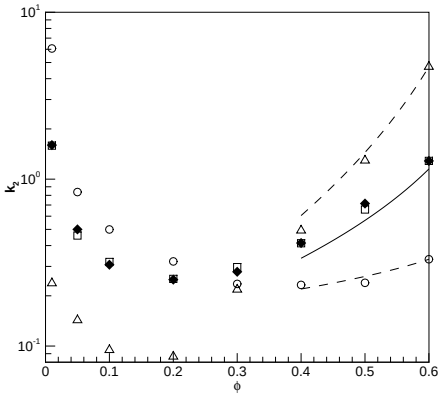

Figure 7: k_2 as function of area fraction ϕ at different values of power- law index: (□), $n = 1$; (Δ), $n = 0.5$ and (◯), $n = 1.5$. The filled diamonds are results for $n = 1$ by Koch and Ladd [5]. The dashed lines are a lubrication theory where we have used the numerical simulation result at $\phi = 0.6$ to obtain the proportionality constant.

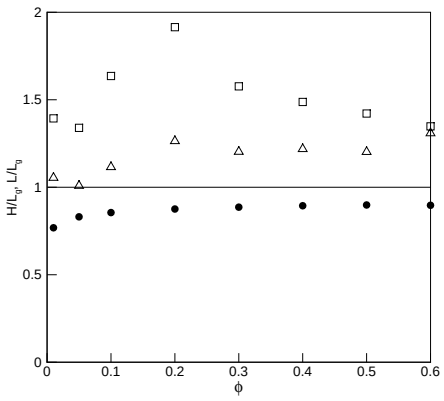

Figure 8: Effective length H which is used in the scaling of the Reynolds number for power-law fluids to obtain a dimensionless inertial contribution to the drag that is independent of the power-law index. (□), $n = 0.5$; (Δ), $n = 1.5$; (•), the length scale L, which yields a drag coefficient for creeping flows that is independent of n. L_g is the minimum size of the gap between the cylinders.

[2] Drummond, J.E. and Tahir, M.I.,Laminar viscous flow through regular arrays of parallel solid cylinders, *Int. J. Multiphase Flow*, **10**, 1984, 515–540.

[3] Edwards, D.A., Shapiro, M., Bar-Yoseph, P. and Shapira, M., The influence of Reynolds number upon the apparant permeability of spatially periodic arrays of cylinders, *Phys. Fluids A*, **2**, 1990, pp.45-55.

[4] Ghaddar, C.K., On the permeability of unidirectional fibrous media: a parallel computational approach, *Phys. Fluids*, **7**, 1995, pp.2563-2586

[5] Koch, D.L. and Ladd, A.J.C., Moderate Reynolds number flows through periodic and random arrays of aligned cylinders, *J. Fluid Mech.*, **349**, 1997, 31–66.

[6] Sadiq, T.A.K., Advani, S.G. and Parnas, R.S., Experimental investigation of transverse flow through aligned cylinders, *Int. J. Multiphase Flow*, **21**, 1995, 755–774.

[7] Sangani, A.S. and Acrivos, A., Slow flow past periodic arrays of cylinders with application to heat transfer, *Int. J. Multiphase Flow*, **8**, 1982, 193–206.

[8] Schowalter, W.R. *Mechanics of Non-Newtonian Fluids* Pergamon, 1978.

[9] Spelt, P.D.M., Selerland, T., Lawrence, C.J. and Lee, P.D., Flows of inelastic non-Newtonian fluids through arrays of aligned cylinders. Part 1. Creeping flows, submitted to *J. Fluid Mech.*, 2001.

[10] Spelt, P.D.M., Selerland, T., Lawrence, C.J. and Lee, P.D., Flows of inelastic non-Newtonian fluids through arrays of aligned cylinders. Part 2. Inertial effects, submitted to *J. Fluid Mech.*, 2001.

[11] Tanner, R.I., Stokes paradox for power-law flow around a cylinder, *J. Non-Newt. Fluid Mech.*, **50**, 1993, 217–224.

[12] Vijaysri, M., Chhabra, R.P and Eswaran, V., Power-law fluid flows across an array of infinite circular cylinders: a numerical study, *J. non-Newt. Fluid Mech.* **87**, 263-282 (1999).

[13] Woods, J.K., Spelt, P.D.M., Lee, P.D., Selerland, T. and Lawrence, C.J., Transverse flow of power-law fluids through a periodic array of ellipsoid shaped tows at low Reynolds number, To be submitted to *Composites A*.

[14] Zang, Y., Street, R.L. and Koseff, J.R., A non-staggered grid, fractional step method for time-dependent incompressible Navier-Stokes equations in curvilinear coordinates, *J. Comp. Phys.*, **114**, 18–33 (1994).